Applied Catalysis A: General 522 (2016) 101–108

Contents lists available at ScienceDirect

Applied Catalysis A: General

journal homepage: www.elsevier.com/locate/apcata

# Silylated layered double hydroxide nanosheets prepared by a large-scale synthesis method as hosts for intercalation of metal complexes

Wenya Guo [a], Yuan Zhao [a], Fan Zhou [a], Xiaoliang Yan [a], Binbin Fan [a,*], Ruifeng Li [a,b,**]

[a] College of Chemistry and Chemical Engineering, Taiyuan University of Technology, Taiyuan 030024, PR China
[b] Key Laboratory of Coal Science and Technology MOE, Taiyuan University of Technology, Taiyuan 030024, PR China

ARTICLE INFO

*Article history:*
Received 22 December 2015
Received in revised form 29 April 2016
Accepted 1 May 2016
Available online 2 May 2016

*Keywords:*
Layered double hydroxide
Nanosheets
Silylation
Metal complexes
Alkene oxidation

ABSTRACT

We present a novel strategy for preparing silylated MgAl layered double hydroxide (LDH) intercalated with metal complexes with the purpose of improving the catalytic activity of the intercalated active species. This strategy involves preparing the exfoliated LDH nanosheets by a large-scale synthesis method, grafting phenyltriethoxysilane (PTES) on the exfoliated LDH nanosheets followed by intercalating the anionic metal complexes such as $CuBDACl_2$ anions ($H_2BDA$, 2, 2′-bipyridine-5, 5′-dicarboxylic acid). The physicochemical properties of the hybrid materials were characterized by X-ray diffraction (XRD), Fourier-transformed infrared spectroscopy (FT-IR), diffuse reflectance ultraviolet-visible spectroscopy (DR UV-–vis), $N_2$ adsorption-desorption, scanning electron microscopy (SEM), and inductively coupled plasma (ICP) techniques. The silane grafted on LDH nanosheets was found to affect the single layer restack while intercalating anionic Cu complexes in water-containing systems. Thus, the resultant hybrid material (PTES-LDH-BDA/Cu) exhibited higher surface area, pore volume and hydrophobicity than its corresponding non-silylated counterpart (LDH-BDA/Cu). These characteristics improved the accessibility of the intercalated $CuBDACl_2$ anions, thus increased their catalytic efficiency in alkene oxidation with *tert*-butyl hydroperoxide (TBHP). In addition, the prepared PTES-LDH-BDA/Cu material exhibited higher reusability as compared to the non-silylated LDH-BDA/Cu material.



## 1. Introduction

With strong striving for an economical and green chemical transformation, considerable attention has been paid on immobilization of catalytically relevant metal complexes on suitable supports [1–3]. The immobilization of homogeneous metal complexes is an interesting method in that it allows easy separation from the reaction media, efficient recycling, superior handling control, and minimization of metal traces in reaction products. Many metal complexes have been successfully immobilized on various polymers or inorganic supports. Compared with organic polymers, inorganic supports are preferred because of their mechanical and thermal stability. Thus, many inorganic materials such as activated carbons [4–6], zeolites [7], and mesoporous materials [8,9] have been employed as supports for the immobilization of a variety of metal complexes. Nevertheless, heterogeneous catalysts usually exhibit lower activity and selectivity than their homogeneous counterparts because of poor dispersion of active sites, steric hindrance effects, and changes in the chemical microenvironment of the active sites. Therefore, novel supports and immobilization strategies are required for the development of efficient heterogeneous catalysts.

Layered double hydroxides (LDHs) are a class of layered materials with the general formula of $[M_{1-x}^{2+}M_x^{3+}(OH)_2]^{x+}[A^{n-}]_{x/n}\cdot yH_2O$ formed by brucite-type octahedral layers in which $M^{2+}$ ions are partially substituted by $M^{3+}$ ions. The net positive charge resulting from this substitution is counterbalanced by exchangeable anions (i.e., interlayer anions) [10–12]. LDHs are composed of two-dimensional positively charged host lattices with excellent anion exchange capacity. These unique structural properties (not shown by conventional zeolite and mesoporous materials) make LDHs promising intercalation hosts for anionic metal complexes. Thus, Fe(III) porphyrin [13–16], Ti(IV)-Schiff base [17], chiral sulphonato-salen-manganese(III) [18], and Ti(IV) tartrate [19,20] have been

* Corresponding author.
** Corresponding author at: Key Laboratory of Coal Science and Technology MOE, Taiyuan University of Technology, Taiyuan 030024, PR China.
*E-mail addresses:* fanbinbin@tyut.edu.cn, fanbinbin@tyut.edu.cn (B. Fan), rfli@tyut.edu.cn (R. Li).

http://dx.doi.org/10.1016/j.apcata.2016.05.001
0926-860X/

successfully intercalated into LDHs and subsequently used as catalysts in a number of reactions (e.g., cyclohexane oxidation, enantioselective hydrogenation, sulfoxidation). Remarkably, the intercalation of metal complexes has been demonstrated to result in materials with enhanced catalytic performance (i.e., activity, selectivity, and stability). However, the strong interaction between the metal hydroxide layers and the interlayer anions can often hinder bulky metal complex anions from gaining access to the interlayer space. This issue can be solved by exfoliation of LDHs into a completely open single interlayer showing no steric hindrance for the immobilization of macromolecules. However, LDHs are exfoliated with difficulty because of the high formal charge density and the strong interaction between adjacent layers [21,22]. Exfoliation of LDHs generally involves the following steps: (i) inserting an anion into the interlayer space; (ii) increasing the distance between the adjacent LDH layers by swelling with an appropriate solvent; and (iii) exfoliating the swollen LDH structure by energy input in an appropriate solvent/dispersant medium [22,23]. This method typically suffers from high solvent consumption and difficult isolation of the exfoliated LDH nanosheets from the solvent dispersion while avoiding aggregation. These issues have dramatically limited the commercial exploitation of LDH nanosheets. Recently, a new aqueous miscible organic solvent treatment (AMOST) method has been developed for the large-scale high yield synthesis of highly porous dispersed LDH powders containing exfoliated nanosheets [24]. The AMOST synthesis involves initial formation of LDHs by conventional co-precipitation and subsequent re-dispersion in an aqueous miscible organic solvent before the final isolation of the solid. This method provides a new opportunity for the application of LDH nanosheets as catalyst supports. However, exfoliated LDHs readily reconstruct into their original layered structure while intercalating anionic metal complexes, leading to hybrid materials with low surface area, pore volume, and low accessibility of the intercalated active species. Hence, it is desirable to find a solution to prevent the exfoliated LDH layers from reconstructing during the immobilization of the anionic metal complexes.

In this work, a novel strategy for preparing silylated LDH intercalated with metal complexes is proposed with the aim of enhancing the catalytic activity of the intercalated active species. This strategy involves initial grafting phenyltriethoxysilane (PTES) on the surface of the exfoliated LDH nanosheets (LHD-del) to generate silylated material (PTES-LDH) and subsequent intercalation of anionic metal complexes such as $CuBDACl_2$ anions ($H_2BDA$: 2, 2′-bipyridine-5, 5′-dicarboxylic acid). The as-prepared hybrid materials were characterized by various techniques and their catalytic performances were investigated in alkene oxidation with *tert*-butylhydroperoxide (TBHP) as the oxidant.

## 2. Experimantal

All chemicals were used as received without further purification.

### 2.1. Sample preparation

LDH nanosheets were prepared according to the AMOST method reported in the literature [24]. Typically, 40 mL of aqueous solution of $Mg(NO_3)_2{\cdot}6H_2O$ (30 mmol) and $Al(NO_3)_3{\cdot}9H_2O$ (10 mmol) was dropped into 100 mL of $H_3BO_3$ solution under vigorous stirring. The pH of the mixture was maintained at 9 by 1.5 M NaOH solution. The resultant gel-like slurry was stirred at room temperature for 10 min and then aged at 65 °C for 12 h. After filtration, the obtained solid was washed with distilled deionized (DD) water until neutral, and then the white slurry was washed by acetone several times and dried at 65 °C overnight. The obtained sample was denoted as LDH-del.

Silylated LDH nanosheets were prepared according to the literature with some modification [25]. 30 mL of toluene was added to 1 g of LDH-del under flowing Ar. After stirring for 0.5 h, 2.95 mmol of phenyltriethoxysilane (PTES) dissolved in 20 mL of toluene was added and the mixture was refluxed for 12 h. The solid product was Soxhlet-extracted with ethanol for 24 h and then dried at 80 °C overnight. The obtained sample was denoted as PTES-LDH.

The intercalation of $CuBDACl_2$ anions was carried out following the procedure reported in the literature [26]. Typically, two equivalents of KOH in DD water (20 mL) were added to a suspension of $H_2BDA$ (2.5 mmol) in 25 mL of *N*,*N*-dimethylformamide (DMF) at 70 °C with stirring under flowing Ar. Subsequently, 1.0 g of LDH-del or PTES-LDH was added and the resulting mixture was stirred at 50 °C for 48 h under flowing Ar. The generated solid was separated by centrifugation, washed several times with ethanol, and vacuum dried at 40 °C for 5 h. The obtained products were denoted as LDH-BDA and PTES-LDH-BDA, respectively.

LDH-BDA or PTES-LDH-BDA (0.8 g) was added to 40 mL ethanol solution of $CuCl_2{\cdot}2H_2O$ (0.025 M) and the resulting suspension was stirred at 30 °C for 19 h. The pale bluish green solid obtained by centrifugation was Soxhlet-extracted with ethanol for 24 h and then dried at 70 °C under vacuum. The obtained catalysts were denoted as LDH-BDA/Cu and PTES-LDH-BDA/Cu, respectively.

The $Cu(H_2BDA)Cl_2$ complex was synthesized as described elsewhere [27]. Briefly, 1 equivalent of $H_2BDA$ (2.5 mmol) and a few drops of hydrochloric acid were added to 50 mL of DMF, and then the mixture was stirred at 70 °C until $H_2BDA$ was completely dissolved. The as-prepared solution was added to 15 mL of ethanol containing 1 equivalent of $CuCl_2{\cdot}2H_2O$ (2.5 mmol) and the resulting mixture was stirred for 2 h at room temperature (RT). The solution was kept at −10 °C until formation of a blue precipitate. After removal of the solvent, the solid was washed with ethanol and vacuum dried at 40 °C for 5 h.

### 2.2. Characterization

Powder X-ray diffraction (XRD) measurement was performed on a Shimazu XRD-6000 diffractometer by using Cu Kα radiation over a $2\theta$ range from 2 to 65°. Fourier-transformed infrared spectroscopy (FT-IR) spectra were recorded by a SHIMADZU FTIR-Affinity-1 spectrometer using the conventional KBr pellet method. Diffuse reflectance UV–vis (DR UV–vis) spectra were recorded using a Cary-300 Absorption Spectrometer. Physisorption of $N_2$ was performed at 77 K using a Quantachrone Nova 1200e and the sample was evacuated at 150 °C for 3 h before measurement. The surface area was calculated by the BET method and the pore distribution was calculated by the BJH method. The Cu and Si contents of the samples were measured by IRIS intrepid II inductively coupled plasma (ICP) atomic emission spectrometer. Mg and Al contents of the samples were measured by energy dispersive X-ray (EDX) on a field-emitting HITACHI S-4800 scanning electron microscope. Thermogravimetrical analysis (TGA) was carried out on a STA 449 F3 thermogravimetrical analyzer from NETZSCH with the sample held in a ceramic pan in a flowing air (10 mL/min). Samples were heated from RT up to 650 °C with a heating rate of 10 °C/min. The contact angles were measured using a KINO SL200B standard optical contact angle measurer. All samples were pressed into disks with a diameter of 14 mm and a thickness of 0.4 mm. The deionized water drops with 5 mL were used in the measurement. Observing all water drops maintained for 20 s, and the measurement for each sample was repeated 3 times. C and N contents in the samples were measured by a Vario EL/micro cube elemental analyzer.

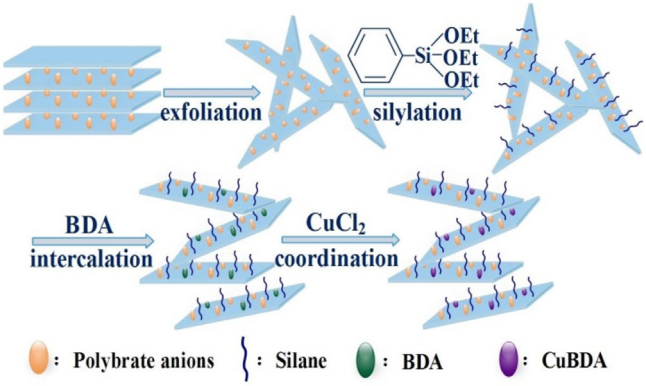


**Scheme 1.** The strategy for the preparation of silylated LDHs intercalated with anionic Cu complexes.

### 2.3. Catalytic reaction

Alkene oxidation was carried out in a 25 mL round bottle flask fitted with water cooled condenser. *tert*-butyl hydroperoxide (TBHP, 70% in aqueous solution) was used as the oxidant. Typically, 10 mmol of substrate was mixed with 5 mL of acetonitrile solvent, and to that 25 mg of catalyst was added. After the reaction mixture was heated to 35 °C in a water bath with vigorous stirring, 1.4 mL of TBHP (10 mmol) was then added and kept at this temperature for 12 h. The liquid products were identified by a GCMS-QP2010 SE and analyzed using a SHIMADZU GC-2014 equipped with a FID detector and a RTX-1 capillary column.

## 3. Results and discussion

### 3.1. Characterization

#### 3.1.1. XRD

MgAl LDH nanosheets were prepared by the reported AMOST method. Intercalation of anionic Cu complexes was carried out by the following two steps: (i) BDA anions were absorbed on the prepared or silylated MgAl LDH nanosheets by ion-exchange; (ii) the resulted LDH-BDA or PTES-LDH-BDA was used as solid ligands to coordinate with $CuCl_2$ in ethanol. The detailed preparation route is illustrated in Scheme1. Fig. 1 shows the XRD patterns of the prepared different samples. No 00*l* reflections were observed in the XRD pattern of LDH-del but 012 and 110/113 reflections with low intensity appeared. These results are in good agreement with previous reports [24] and indicate that LDH nanosheets were successfully prepared. Remarkably, a new reflection corresponding to the (003) reflection appeared upon addition of BDA anions (LDH-BDA sample) thereby revealing recombination of LDH nanosheets during the intercalation process. The (003) reflection of LDH-BDA, originated from the brucite-like layer stacking, was detected at $2\theta$ value significantly lower as compared to LDHs with tetraborate and nitrate anions ($2\theta = 8$ and 10°, respectively) [28,29]. This shift originated from the intercalation of bulky BDA anions into the restructured LDH interlayer. In order to further confirm the successful intercalation of BDA anions, LDH-re-$H_2O$ was prepared by immersing of LDH-del in water for 24 h. The water-treated sample showed the (003) reflection at $2\theta = 9.5$ and the corresponding basal spacing was 0.93 nm. Subtracting the layer thickness (0.48 nm) from the basal spacing, its interlayer spacing was only 0.45 nm. In contrast, the (003) reflection of LDH-BDA was detected at $2\theta = 4.8°$, resulting in an interlayer spacing (1.36 nm = 1.84 nm–0.48 nm) slightly lower than the longest dimension of the BDA anions (1.42 nm) [30,31]. This lower interlayer spacing (as compared to BDA anion dimension) may arise

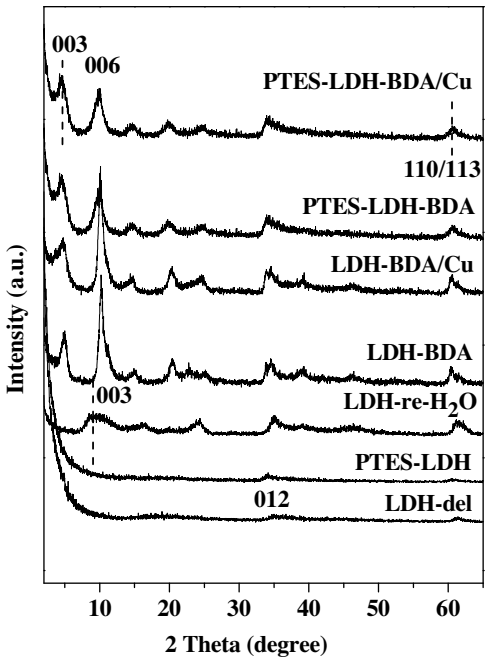


**Fig. 1.** XRD patterns of the prepared different samples.

from: (i) BDA anions slightly tilted (i.e., not perpendicular) to the host layers; (ii) a strong hydrogen bond between the carboxylate groups in the BDA anions and the brucite-like layers (as revealed by TG results below). An unexpectedly sharp and intense reflection at $2\theta = 10°$ was also observed in the case of LDH-BDA. Since LDH-del was synthesized in the system containing $NO_3^-$ and $[B_4O_5(OH)_4]^{2-}$ anions, the resulting LDH-BDA may contain two segregated phases, one containing only $NO_3^-$ (LDH-$NO_3^-$) and the other containing BDA anions and $NO_3^-/[B_4O_5(OH)_4]^{2-}$. Accordingly, the sharp and intense reflection at $2\theta = 10°$ may result from the overlap of the (003) and (006) reflections from the two segregated phases. Neatu et al. observed a similar phenomenon during immobilization of $Rh(TPPTS)_3Cl$ on LDHs by anionic exchange [29]. After coordinating with $CuCl_2$, the obtained LDH-BDA/Cu showed nearly similar XRD pattern to LDH-BDA. Remarkably, the PTES-LDH sample, prepared by refluxing LDH-del with a PTES toluene solution, displayed nearly identical XRD pattern as compared to LDH-del, thereby indicating that the silane modification had little influence on the layered structure of the original LDH nanosheets. In the same way, PTES-LDH-BDA exhibited similar XRD pattern to the LDH-BDA sample. Moreover, unlike LDH-BDA, PTES-LDH-BDA showed the reflection at $2\theta = 10°$ with normal intensity compared to other reflections, revealing that PTES-LDH-BDA mostly consists of the phase containing BDA anions and $NO_3^-/[B_4O_5(OH)_4]^{2-}$ and the dispersion of BDA anions in PTES-LDH-BDA is higher than that in LDH-BDA. After coordinating with $CuCl_2$, the obtained PTES-LDH-BDA/Cu also showed nearly identical XRD pattern as compared to PTES-LDH-BDA.

#### 3.1.2. FTIR and DR UV-vis

The successful graft of PTES and the intercalation of the $CuBDACl_2$ anions into LDHs can be further testified by FTIR and DR UV–vis. The FTIR spectra of the prepared samples are shown in Fig. 2. The broad band at 3446 $cm^{-1}$ was attributed to the O—H stretching vibration of hydroxyl groups in the brucite-like layers and water in the galleries. LDH-del and PTES-LDH showed an intense sharp band at 1385 $cm^{-1}$ attributed to the $\nu 3$ stretching vibration of nitrate [32]. Compared with LDH-del, some new bands were observed in the FTIR spectrum of the PTES-LDH, in which the band at 1040 $cm^{-1}$ is attributed to the stretching vibration of Si-

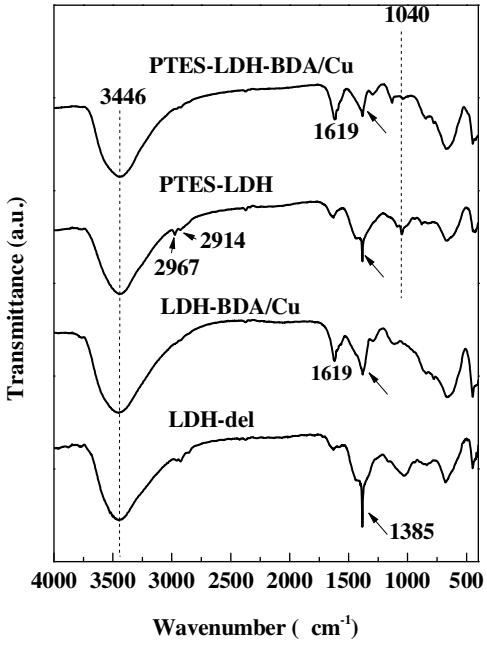


**Fig. 2.** FTIR spectra of the prepared different samples.

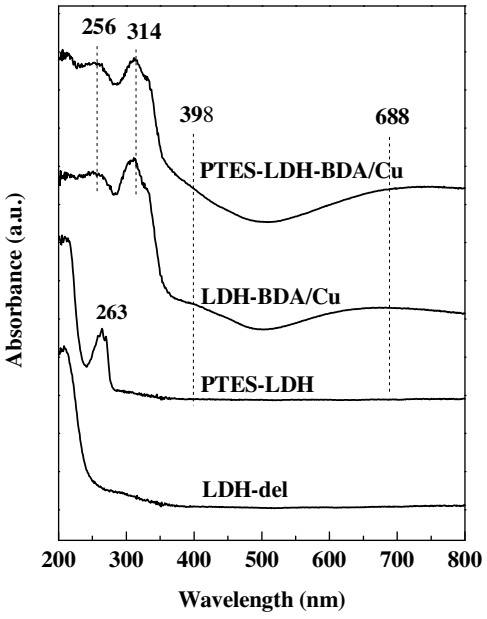


**Fig. 3.** DR UV–vis spectra of the prepared different samples.

O bond and the bands at 2967 $cm^{-1}$ and 2914 $cm^{-1}$ are ascribed to the vibrations of $CH_3$-, $-CH_2$- groups from EtO- in the PTES [33–35]. These results reveal that PTES was successfully grafted on the LDH nanosheet surface by Mg(Al)—O—Si bonds (i.e., single, double, or triple bond). Intercalation of $CuBDACl_2$ anions resulted in the onset of a new band at 1619 $cm^{-1}$ (detected in both LDH-BDA/Cu and PTES-LDH-BDA/Cu samples) attributed to the asymmetric stretching vibrations of the carboxylate groups. These results confirmed the presence of BDA anions in the LDH materials.

The DR UV–vis spectra of the different samples under study are shown in Fig. 3. LDH-BDA/Cu and PTES-BDA/Cu were light green whereas the LDH support was white colored. Unlike LDH-del, PTES-LDH showed an intense peak at 263 nm assigned to the benzoic ring of PTES [36] thereby confirming the successful silane graft. Intercalation of $CuBDACl_2$ anions was accompanied by the onset of two new bands at 256 and 314 nm ascribed to the $\pi$-$\pi^*$ transition of the ligand BDA [37]. These bands were observed for both LDH-BDA/Cu and PTES-LDH-BDA/Cu samples, indicating that BDA anions were ion-exchanged into the interlayer of the restacked LDH. Additionally, these two samples showed a weak shoulder at ca 398 nm and a broad band at ca 688 nm that were ascribed to the ligand-to-metal charge transfer and d–d electronic transitions, respectively [26], thereby demonstrating that intercalated BDA anions were successfully coordinated with $CuCl_2$.

**Table 1**
The surface areas and pore volumes of the prepared different samples.

| Sample | BET surface area ($m^2$/g) | Pore volume ($cm^3$/g) |
|---|---|---|
| LDH-del | 233 | 0.617 |
| LDH-BDA/Cu | 61 | 0.309 |
| PTES-LDH | 242 | 0.934 |
| PTES-LDH-BDA/Cu | 199 | 0.766 |

### 3.1.3. $N_2$ adsorption isotherms

The textural properties of the samples under study were investigated by $N_2$ adsorption-desorption isotherms (Fig. 4). From Fig. 4(A), it can be seen that all the samples showed a type IV adsorption isotherm with a H3 hysteresis loop indicating the presence of plate-like particles giving rise to slit-shaped pores. The onset of the hysteresis loop started at ca 0.8 and 0.6 relative pressure for PTES-LDH and LDH-del, respectively. Thus, the grafted silane influenced the pores between the exfoliated layers with PTES-LDH showing larger pore size than LDH-del (Fig. 4(B)). After intercalation of $CuBDACl_2$ anions, the specific surface area and pore volume of LDH-BDA/Cu decreased significantly as compared to its precursor host (Table 1). This decrease in textural properties is mainly explained by the reconstruction of the exfoliated LDH nanosheets while intercalating anionic BDA ligands in the water-containing system. The same trend was observed for PTES-BDA/Cu to a much lower extent as compared to LDH-BDA/Cu (Table 1). This behavior might be associated to: (i) grafted PTES increasing the hydrophobicity of LDH nanosheets and thereby partially hindering their restack; (ii) grafted PTES increasing the extent of particle crosslinking with the corresponding increase in mesopore volume [33]; and (iii) LDH-BDA/Cu being enriched in LDH-$NO_3^-$ phase as compared to PTES-LDH-BDA/Cu. Remarkably, the hypothesis (i) was confirmed by water contact angles measurements (LDH-BDA/Cu: 57.3°, while PTES-BDA/Cu: 79.3°).

### 3.1.4. TG analysis

As shown in Fig. 5, the TG curves of LDHs are typically composed of three losses, namely, desorption of physically adsorbed water or acetone (from RT to 150 °C), dehydroxylation of the brucite-like sheets (150–290 °C), and decomposition of the interlayer anions/grafted organic silane (T > 290 °C). Dehydroxylation accounted for lower mass losses in silylated samples (5.5 and 5.8% for PTES-LDH and PTES-LDH-BDA/Cu, respectively) as compared to LDH-del (6.7%), potentially revealing lower amounts of —OH groups in the PTES-LDH nanosheets as a result of the condensation reaction [35]. The neat $Cu(H_2BDA)Cl_2$ complex decomposed at ca 300 °C (insert graph), while this temperature shifted to higher values (350 °C) after intercalation. The formation of strong hydrogen bonds between the carbonyl oxygen atoms of coordinated carboxylate groups and the LDH layers can explain this phenomenon [38].

### 3.1.5. Elemental analysis

As measured by SEM coupled with energy-dispersive X-ray spectroscopy (EDX), the prepared LDH nanosheets showed a Mg/Al molar ratio of 2.2 (theoretical value: 3) that remained nearly

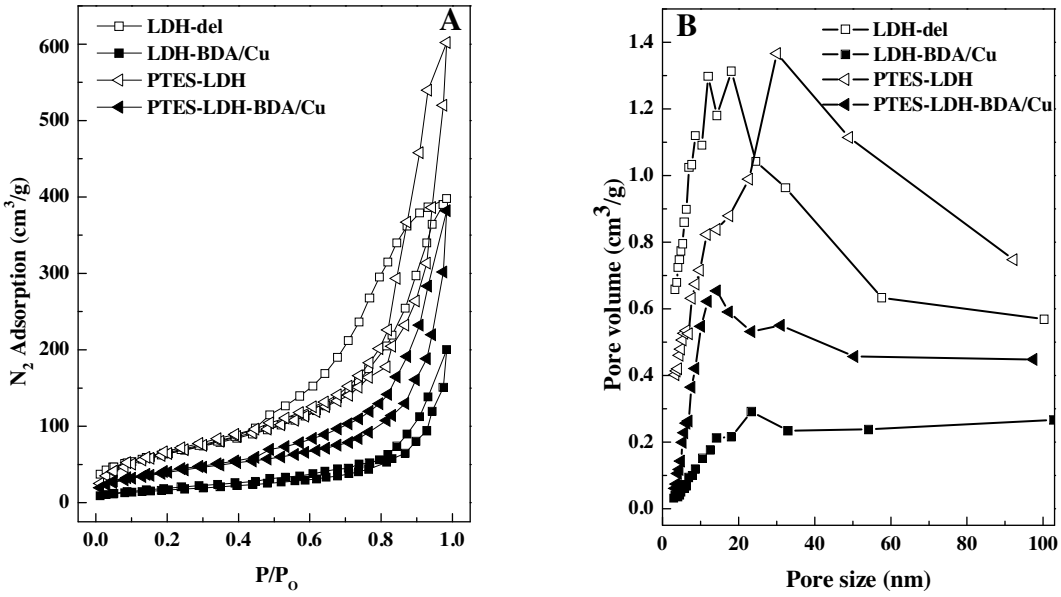


**Fig. 4.** $N_2$ adsorption/desorption isotherms (A) and pore size distributions (B) of the prepared different samples.

**Table 2**
The Si and Cu contents of the samples prepared under different conditions.

| Entry | Sample | PTES/LDH (mmol/g) | BDA/LDH (mmol/g) | Si (mmol/g) | Cu (mmol/g) | C (wt%) | N (wt%) |
|---|---|---|---|---|---|---|---|
| 1 | LDH-BDA/Cu | – | 2.5 | 0 | 1.133 | 16.32 | 3.59 |
| 2 | PTES-LDH-BDA/Cu-1 | 1.48 | 2.5 | 0.189 | 0.704 | 12.35 | 2.17 |
| 3 | PTES-LDH-BDA/Cu | 2.95 | 2.5 | 0.384 | 0.656 | 13.17 | 1.95 |
| 4 | PTES-LDH-BDA/Cu-2 | 5.91 | 2.5 | 0.643 | 0.636 | 15.61 | 1.84 |
| 5 | PTES-LDH-BDA/Cu-3 | 2.95 | 1.0 | 0.384 | 0.457 | 10.39 | 1.31 |
| 6 | PTES-LDH-BDA/Cu-4 | 2.95 | 5.0 | 0.384 | 1.055 | 15.84 | 3.38 |
| 7 | PTES-LDH-BDA/Cu-5 | 2.95 | 10.0 | 0.384 | 1.278 | 22.2 | 3.67 |
| 8 | LDH-del | – | – | – | – | 0.45 | 1.81 |
| 9 | LDH-BDA | – | 2.5 | – | – | 16.53 | 3.61 |
| 10 | PTES-LDH | 2.95 | – | 0.384 | – | 3.86 | 1.02 |

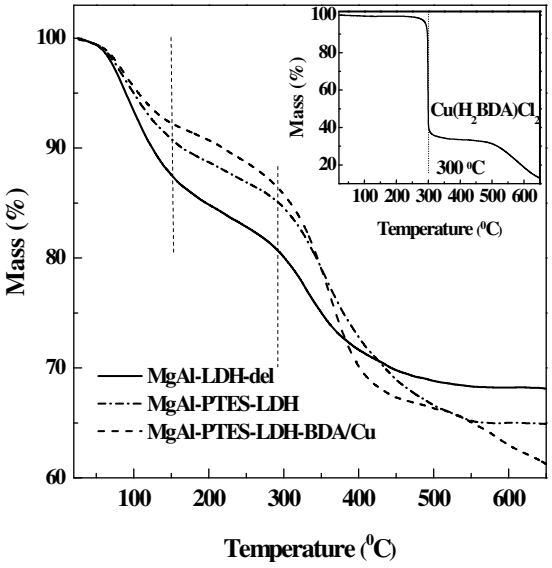


**Fig. 5.** TG curves of the prepared different catalysts.

unchanged after PTES grafting and $CuBDACl_2$ intercalating processes. The Cu and Si contents of the samples were measured by ICP (Table 2). PTES-LDH-BDA/Cu samples with varying amounts of PTES and BDA anions were prepared by varying the PTES or BDA concentration in toluene or DMF solution. From Table 2, it can be clearly seen that the silylation process strongly affected the amount of intercalated $CuBDACl_2$ anions. The Cu content in the PTES-LDH-BDA/Cu was lower than that in the corresponding LDH-BDA/Cu, and the Cu content decreased with the PTES loading (Table 2, Entry 1–4). As indicated above, intercalation of $CuBDACl_2$ anions involves the following steps: (i) adsorption of BDA anions on the prepared or silylated MgAl LDH nanosheets via ion-exchange of the nitrate or polyborate anions; and (ii) coordination of $CuCl_2$ with intercalated BDA anions. The first step is crucial and it determines the final amount of intercalated $CuBDACl_2$ anions. Thus, the higher hydrophobicity of the silylated samples might influence the interaction of BDA anions with the LDH layers, thereby resulting in less BDA anions being incorporated into the reconstructed LDH interlayer. In addition, the concentration of BDA anions in the ion-exchange solution can also influence the amount of intercalated $CuBDACl_2$ anions. Thus, the Cu content was tailored to some extent by varying the BDA concentration of the ion-exchange solution (Table 2, Entry 4–7).

The C and N microanalysis for the different samples are also listed in Table 2. The C (from atmospheric $CO_2$ adsorption) and N (from nitrate ions) contents in LDH-del were 0.45 and 1.81%, respectively. PTES-LDH showed higher C content as compared to LDH-del, with the amount of C exceeding the theoretical value (based on Si content and no residual EtO- groups). This result reveals some PTES to be grafted on LDH nanosheets by single or double Mg(Al)—O—Si bonds. The N contents in all $CuBDACl_2$-

**Table 3**
Catalytic results obtained over the different samples in styrene oxidation with TBHP.

| Entry | Sample | Conversion (%) | Selectivity (%) | | | TON[b] |
|---|---|---|---|---|---|---|
| | | | BA[a] | SO[a] | others | |
| 1 | PTES-LDH | 1.6 | 76.2 | 19.9 | 3.9 | – |
| 2 | CuBDA | 3.9 | 73.1 | 21.5 | 5.4 | 14.2 |
| 3 | CuBDA+ PTES-LDH | 4.5 | 70.6 | 25.3 | 4.1 | 14.7 |
| 4 | LDH-BDA/Cu | 18.8 | 64.6 | 25.0 | 10.4 | 66.4 |
| 5 | PTES-LDH-BDA/Cu-1 | 19.7 | 65.4 | 31.4 | 3.2 | 111.9 |
| 6 | PTES-LDH-BDA/Cu | 25.8 | 65.9 | 31.5 | 2.6 | 157.3 |
| 7 | PTES-LDH-BDA/Cu-2 | 25.4 | 65.0 | 31.3 | 3.7 | 159.7 |
| 8 | PTES-LDH-BDA/Cu-3 | 17.9 | 65.3 | 31.8 | 2.9 | 158.0 |
| 9 | PTES-LDH-BDA/Cu-4 | 28.6 | 63.4 | 34.1 | 2.5 | 108.4 |
| 10 | PTES-LDH-BDA/Cu-5 | 31.8 | 58.1 | 37.9 | 4.0 | 99.5 |

Reaction condition: catalyst 25 mg, styrene 10 mmol, TBHP aqueous 10 mmol, acetonitrile 5 mL, 35 °C, 12 h.
[a] BA: benzaldehyde, SO: styrene oxide.
[b] TON: mmol of converted substrate per mmol of copper content in the catalyst for 12 h.

containing samples were slightly higher than those calculated based on the Cu content. This is due to that ion-exchange of nitrate anions in LDH-del with BDA anions was incomplete. Therefore, the C and N contents are not proper indication of the Cu/BDA ratio in the samples. The BDA loading can be roughly estimated in PTES-LDH-BDA/Cu by deducting the C content of PTES-LDH, resulting in a Cu/BDA molar ratio close to 1.

### 3.2. Catalytic reaction

#### 3.2.1. Catalytic performance of the prepared samples

Table 3 summarizes the catalytic performance of the prepared samples in the oxidation of styrene with TBHP. Benzaldehyde was the main product along with styrene oxide. Minor amounts of benzoic acid and phenylacetaldehyde were produced during the course of the reaction. PTES-LDH showed very low styrene conversion (1.6%, Table 3, Entry 1) as compared to $CuBDACl_2$-containing samples (LDH-BDA/Cu: 18.8%; PTES-LDH-BDA/Cu: 25.8% (Table 3, Entry 4–6), thereby indicating that $CuBDACl_2$ anions are the active species for styrene oxidation. Neat $Cu(H_2BDA)Cl_2$ and a physical mixture of silylated LDHs and $Cu(H_2BDA)Cl_2$ (containing the same amount of $CuBDACl_2$ as the heterogeneous counterpart) showed very low conversions (3.9 and 4.5%, respectively, Table 3, entry 2 and 3), as expected by the insolubility of the Cu complex in reaction medium. In contrast, intercalation of $CuBDACl_2$ anions into LDH effectively increased its dispersion thus greatly improving the catalytic performance. LDHs are weak bases and can thus assist in the cleavage of the peroxide bond in TBHP [36,39] thereby enhancing the oxidation capacity of TBHP. Compared with LDH-BDA/Cu, PTES-LDH-BDA/Cu showed higher activity and TON value. Based on the characterization results, this result can be explained by: (i) the higher dispersion of $CuBDACl_2$ anions in PTES-LDH-BDA/Cu as compared to LDH-BDA/Cu increased the accessibility of the intercalated $CuBDACl_2$ to the substrate; (ii) the higher surface area and pore volume of silylated samples were beneficial to the diffusion of the substrates and reaction products; and (iii) the higher hydrophobicity of PTES-LDH-BDA/Cu was favorable for styrene adsorption and the main product desorption, because benzaldehyde is more polar than styrene. The amount of grafted PTES and intercalated $CuBDACl_2$ anions also influenced the catalytic performance (Table 3). The TON value enhanced with the PTES loading (Table 3, Entry 4–7) up to 0.384 mmol/g and leveled off thereafter (Table 3, Entry 7). The styrene conversion increased with the amount of intercalated $CuBDACl_2$ anions, although the corresponding TON values decreased (Table 3, Entry 6, 8–10).

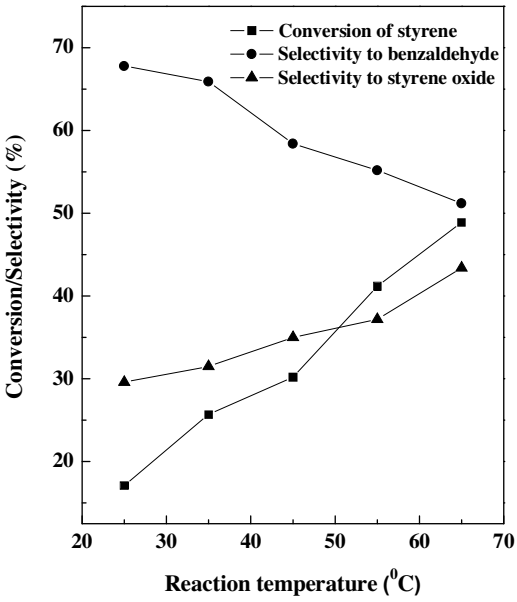


**Fig. 6.** Effect of reaction temperature on the catalytic performance of PTES-LDH-BDA/Cu (Reaction conditions: catalyst 25 mg, styrene 10 mmol, TBHP 10 mmol, acetonitrile 5 mL, 12 h).

**Table 4**
Catalytic results for alkene oxidation over the different catalysts.

| Substrate | Catalyst | Conversion (%) | Selectivity[a] (%) | TON[b] |
|---|---|---|---|---|
| Cyclohexene | $Cu(H_2BDA)Cl_2$ | 1.8 | 14.8 | 6.6 |
| | LDH-BDA/Cu | 12.8 | 81.2 | 45.2 |
| | PTES-LDH-BDA/Cu | 24.1 | 91.9 | 147.0 |
| Cyclooctene | $Cu(H_2BDA)Cl_2$ | 0.6 | 62.7 | 2.2 |
| | LDH-BDA/Cu | 7.9 | 70.3 | 27.9 |
| | PTES-LDH-BDA/Cu | 14.3 | 77.2 | 87.2 |

Reaction conditions: catalyst 25 mg, substrate 10 mmol, TBHP 10 mmol, acetonitrile 5 mL, 35 °C, 12 h.
[a] The corresponding product selectivity are 2-cyclohexanone and cyclooctene oxide, respectively.
[b] TON: mmol of converted substrate per mmol of copper content in the catalyst for 12 h.

#### 3.2.2. Influence of the reaction temperature

The influence of the reaction temperature over the styrene conversion and product distribution was investigated for PTES-LDH-BDA/Cu. The styrene conversion increased significantly with temperature (Fig. 6). Unlike styrene oxide, the selectivity to benzaldehyde decreased with temperature, being consistent with the reported result [40]. Thus, epoxidation of the C=C bond to styrene oxide is favoured at higher temperatures than the C=C cleavage process leading to benzaldehyde.

#### 3.2.3. Influence of the reaction time

The styrene conversion over LDH-BDA/Cu and PTES-LDH-BDA/Cu gradually increased with time (19.3 and 29.7%, respectively at 24 h and 35 °C, Fig. 7). The product distribution (basically benzaldehyde and styrene oxide, not shown) remained constant throughout the experiment. These results indicate that the two competitive reaction mechanisms (i.e., C=C cleavage and epoxidation) proceeded in parallel at the mild reaction conditions herein used.

#### 3.2.4. Influence of the reaction substrates

The oxidation of cyclohexene and cyclooctene were also investigated and the corresponding results are given in Table 4. As expected, LDH-BDA/Cu and PTES-LDH-BDA/Cu exhibited much higher catalytic activity and TON values than neat $Cu(H_2BDA)Cl_2$.

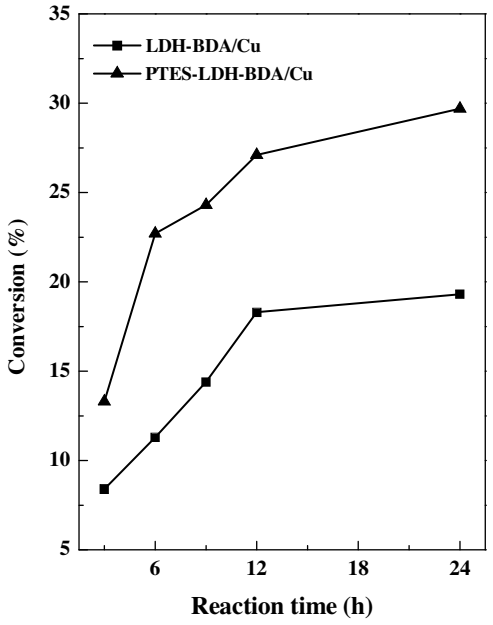


**Fig. 7.** Effect of reaction time on the catalytic performance over LDH-BDA/Cu and PTES-LDH-BDA/Cu (Reaction conditions: catalyst 25 mg, styrene 10 mmol, TBHP 10 mmol, acetonitrile 5 mL, 35 °C).

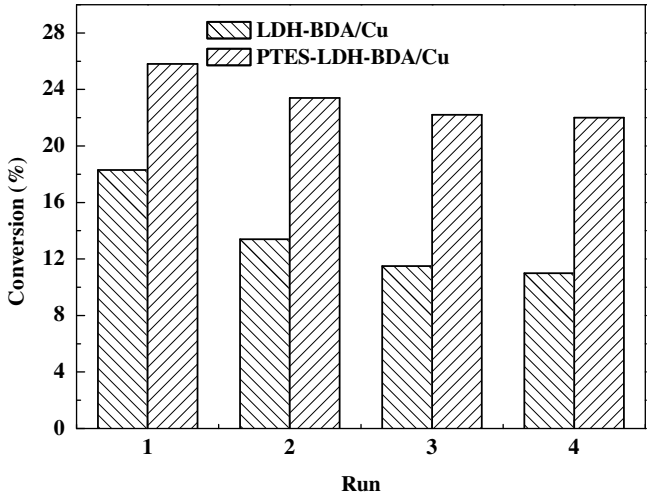


**Fig. 8.** Recycling of LDH-BDA/Cu and PTES-LDH-BDA/Cu for styrene oxidation (Reaction conditions: catalyst 25 mg, styrene 10 mmol, TBHP 10 mmol, acetonitrile 5 mL, 35 °C, 12 h).

The silylated samples showed much higher TON values as compared to non-silylated materials, with this trend being more significant with the substrate size. In addition, the silylated sample gave higher selectivities to 2-cyclohexanone/cyclooctanone than the non-silylated sample.

### 3.2.5. Catalyst stability

The stability of the prepared samples in the styrene oxidation reaction with TBHP was investigated. The catalyst was recovered after each run by centrifugation and subsequent drying before being used for the next run under identical reaction conditions. PTES-LDH-BDA/Cu maintained 78% of its original activity after four successive runs whereas LDH-BDA/Cu retained 60% of its initial activity (Fig. 8). Reasons for the loss in activity with recycling include loss of the very fine particles catalyst, leaching of Cu species and the irreversible deactivation of basic sites by formed benzoic acid in reaction. ICP measurements showed that ca 6% of the Cu loading in LDH-BDA/Cu leached after the first run versus only ca 2.5% for PTES-BDA/Cu. Thus, PTES modification can effectively improve the stability of the intercalated $CuBDACl_2$ anions. To further check the contribution of the leached Cu species, the following experiments were carried out. After finishing the first run, the PTES-LDH-BDA/Cu catalyst was separated from the reaction mixture, and then the substrate and TBHP were added to the filtrate to perform the second run. It was found that the leached Cu species from PTES-LDH-BDA/Cu were nearly inactive during the oxidation of fresh styrene with TBHP (ca 2% conversion).

## 4. Conclusions

Silylated LDH nanosheets were successfully employed as intercalation hosts for metal complexes. The grafted silane greatly affected the restack of the single layer while intercalating $Cu(BDA)Cl_2$ anions in aqueous solution, and the resultant PTES-LDH-BDA/Cu exhibited higher surface and pore volume than its corresponding non-silylated LDH-BDA/Cu counterpart. PTES-LDH-BDA/Cu showed both higher catalytic activity and stability than LDH-BDA/Cu for the styrene oxidation with TBHP. This work provides a novel method for the preparation of heterogeneous catalysts based on LDH hosts.

## Acknowledgements

This work is supported by the National Natural Science Foundation of China (No. 20971095, 21576177) and Research Project Supported by Shanxi Scholarship Council of China (2013-047).

## References

[1] B.M.L. Dioos, I.F.J. Vankelecom, P.A. Jacobs, Adv. Syn. Catal. 348 (2006) 1413–1446.
[2] T.S. Koblenz, J. Wassenaar, J.N.H. Reek, Chem. Soc. Rev. 37 (2008) 247–262.
[3] M.R. Maurya, A. Kumar, J.C. Pessoa, Coord. Chem. Rev. 255 (2011) 2315–2344.
[4] A. Schaetz, M. Zeltner, W.J. Stark, ACS Catal. 2 (2012) 1267–1284.
[5] A.R. Silva, J.L. Figueiredo, C. Freire, B. Castro, Microporous Mesoporous Mater 68 (2004) 83–89.
[6] A.R. Silva, M.M.A. Freitas, C. Freire, B. Castro, J.L. Figueiredo, Langmuir 18 (2002) 8017–8024.
[7] D.J. Xuereb, Catal. Today 198 (2012) 19–34.
[8] C.M.A. Parlett, K. Wilson, A.F. Lee, Chem. Soc. Rev. 42 (2013) 3876–3893.
[9] C. Li, Catal. Rev. 46 (2004) 419–492.
[10] C.M. Li, M. Wei, D.G. Evans, X. Duan, Small 10 (2014) 4469–4486.
[11] G.L. Fan, F. Li, D.G. Evans, X. Duan, Chem. Soc. Rev. 43 (2014) 7040–7066.
[12] S. Nishimura, A. Takagaki, K. Ebitani, Green Chem. 15 (2013) 2026–2042.
[13] M. Halma, K.A.F. Castro, C. Gueho, V. Prévot, C. Forano, F. Wypych, S. Nakagaki, J. Catal. 257 (2008) 233–243.
[14] F. Wypych, A. Bail, M. Halma, S. Nakagaki, J. Catal. 234 (2005) 431–437.
[15] G.S. Machado, G.G.C. Arízaga, F. Wypych, S. Nakagaki, J. Catal. 274 (2010) 130–141.
[16] K.A.F.A. Castro, P.B. Groszewicz, G.S. Machado, W.H. Schreiner, F. Wypych, S. Nakagaki, Appl. Catal. A 386 (2010) 51–59.
[17] K.M. Parida, M. Sahoo, S. Singha, J. Catal. 276 (2010) 161–169.
[18] S. Bhattacharjee, J.A. Anderson, Adv. Synth. Catal. 348 (2006) 151–158.
[19] H.M. Shi, C.G. Yu, J. He, J. Catal. 271 (2010) 79–87.
[20] H.M. Shi, C.G. Yu, J. He, J. Phys. Chem. C 114 (2010) 17819–17828.
[21] Y. Wei, F.C. Li, L. Liu, RSC Adv. 4 (2014) 18044–18051.
[22] Q. Wang, D.O. Hare, Chem. Rev. 112 (2012) 4124–4155.
[23] T. Hibino, J. William, J. Mater. Chem. 11 (2001) 1321–1323.
[24] Q. Wang, D.O. Hare, Chem. Commun. 49 (2013) 6301–6303.
[25] L. Yang, B.B. Fan, X.Y. Cui, X.F. Shi, R.F. Li, J. Ind. Eng. Chem. 21 (2015) 689–695.
[26] B. Monteiro, S. Gago, S.S. Balula, A.A. Valente, I.S. Gonçalves, M. Pillinger, J. Mol. Catal. A 312 (2009) 23–30.
[27] F.P. Canhota, G.C. Salomão, N.M.F. Carvalho, O.A.C. Antunes, Catal. Commun. 9 (2008) 182–185.
[28] L.S. Li, S.J. Ma, X.S. Liu, Y. Yue, J.B. Hui, R.R. Xu, Y.M. Bao, J. Rocha, Chem. Mater. 8 (1996) 204–208.
[29] F. Neaţu, M. Besnea, V. Komvokis, J.P. Genêt, V. Michelet, K. Triantafyllidis, V. Pârvulescu, Catal. Today 139 (2008) 161–167.
[30] D.W. Min, S.S. Yoon, S.W. Lee, Inorg. Chem. Commun. 5 (2002) 143–146.
[31] S. Gago, M. Pillinger, A.A. Valente, T.M. Santos, J. Rocha, I.S. Gonçalves, Inorg. Chem. 43 (2004) 5422–5431.
[32] H. Chai, Y.J. Lin, D.G. Evans, D.Q. Li, Ind. Eng. Chem. Res. 47 (2008) 2855–2860.

[33] Q. Tao, H.P. He, T. Li, R.L. Frost, D. Zhang, Z.S. He, J. Solid State Chem. 213 (2014) 176–181.
[34] Q. Tao, J.X. Zhu, R.M. Wellard, T.E. Bostrom, R.L. Frost, P. Yuan, H.P. He, J. Mater. Chem. 21 (2011) 10711–10719.
[35] Q. Tao, H.P. He, R.L. Frost, P. Yuan, J.X. Zhu, Appl. Surf. Sci. 255 (2009) 4334–4340.
[36] G.D. Wu, X.L. Wang, J.P. Li, N. Zhao, W. Wei, Y.H. Sun, Catal. Today 131 (2008) 402–407.
[37] A.C. Gomes, S.M. Bruno, A.A. Valente, I.S. Gonçalves, M. Pillinger, J. Organomet. Chem. 744 (2013) 53–59.
[38] A.S. Barbosa, D.C. Ferreira, R.L. Constantino, Eur. J. Inorg. Chem. 8 (2005) 1577–1584.
[39] V.R. Choudhary, R. Jha, P. Jana, Green Chem. 8 (2006) 689–690.
[40] C. Saux, L.B. Pierella, Appl. Catal. A 400 (2011) 117–121.